

- quasi-equilibrium between the reactant or reactants and the "transition state," a critical set of configurations from which, once reached, there is no return to the original reactant or reactants but rather the system proceeds to form the product or products. Because of the quasi-equilibrium aspect, concepts such as "free energy of activation" and "statistical mechanical partition function" appear in the canonical (i.e., temperature-based) transition state theory, and concepts such as number of quantum states  $N_{EJ}^{\ddagger}$  in the transition state and density of states  $\rho_{EJ}^{\ddagger}$  of the unimolecularly dissociating or isomerizing molecule appear in its microcanonical counterpart, RRKM theory (Eq. 1). The transition state for the forward reaction is the same as that of the reverse reaction and it occurs at the maximum of a free energy barrier in canonical transition state theory, or at the minimum of an entropy barrier (minimum  $N_{EJ}^{\ddagger}$ ) at the given energy  $E$  and  $J$  in RRKM theory. This maximum or minimum property confers on it the title "variational transition state theory" or "variational RRKM theory."
51. I. Oref, B. S. Rabinovitch, *Acc. Chem. Res.* **12**, 166 (1979), and references cited therein.
52. R. Weinkauff *et al.*, *J. Chem. Phys.* **98**, 8381 (1994); see also (77).
53. S. K. Kim *et al.*, *J. Phys. Chem.* **100**, 9202 (1996).
54. The shaded region for XYZ in Fig. 1 was assumed to be absent in (42). This assumption affects only absolute rates, but has no effect on the ratios of the rate constants, and so no effect on the present Figs. 2 through 4.
55. W. L. Hase, *J. Chem. Phys.* **64**, 2442 (1976).
56. M. Quack, J. Troe, *Ber. Bunsenges. Phys. Chem.* **81**, 329 (1977).
57. G. P. Smith, D. M. Golden, *Int. J. Chem. Kinet.* **10**, 489 (1978).
58. S. J. Klippenstein, R. A. Marcus, *J. Chem. Phys.* **91**, 2280 (1989).
59. For example, G. Lendvay, G. C. Schatz, in *Adv. Chem. Kinet. Dyn.* **2B**, 481 (1995), and references cited therein.
60. J. R. Barker, B. M. Toselli, *Int. Rev. Phys. Chem.* **12**, 305 (1993), and references cited therein.
61. R. G. Gilbert, *Aust. J. Chem.* **48**, 1787 (1995).
62. A. J. Stace, J. N. Murrell, *J. Chem. Phys.* **68**, 3028 (1978).
63. C. Leforestier *et al.*, *J. Chem. Phys.* **101**, 3806 (1994).
64. The need for a barrierless potential-energy surface is reflected in the negative temperature coefficient of the various recombination and isotopic exchange reactions, e.g., in (45) and in (38), and also in Table 1, and in the absolute values of the rate constants given there. Apart from an electronic degeneracy factor, they are near gas-kinetic. The expression in (63) gives, instead, an energy barrier.
65. A. Gross, G. D. Billing, *Chem. Phys.* **217**, 1 (1999).
66. R. A. Marcus, Y. Q. Gao, *J. Chem. Phys.* **114**, 9807 (2001).
67. H. Craig, *Geochim. Cosmochim. Acta* **12**, 133 (1957).
68. Y. Matsuhisa, J. R. Goldsmith, R. N. Clayton, *Geochim. Cosmochim. Acta* **42**, 173 (1978).
69. The  $E^M$  was expressed in (42) in terms of the individually calculated recombination rate constants. To obtain an expression for these enrichments  $E^M$  and  $\delta^{\circ}$  and still allow for the numerous isotopomers of each species, it was noted that certain ratios of statistical mechanical partition functions (not the partitioning factors  $Y!$ ) were equal to unity, within several thousandths (42). This approximation provided a considerable simplification of a large number of reaction equations involving the many permutations of X, Y, and Z and led to simple final expressions in (42) involving individual rate constants  $k_{bi}$  and certain equilibrium constants.
70. For the present calculations of the rate constants and of the enrichments  $E^M$  for the many isotopomers, only 26 of the 54 isotopomeric vibration frequencies were known, and the missing ones were needed in the calculations for densities of states  $\rho_{EJ}^{\ddagger}$ . A second-order perturbation formulation gave the unknown frequencies to an accuracy of about  $1 \text{ cm}^{-1}$ , quite sufficient for the present purpose (78). The long-range part of the interaction potential  $-C_6/r^6$  was used in the calculation of the potential-energy surface, in addition to the short-range potential terms,  $C_6$  being obtained from collision cross sections for  $\text{O} + \text{O}_2$  (79). The anharmonicity effect on the density of states  $\rho_{EJ}^{\ddagger}$  was obtained from vibrational spectra of ozone molecules (80), by fitting those data to a theoretical expression containing the various anharmonicity constants (49). The various enrichments and rate constants were calculated using the relevant equations given in (42, 43) but now using the presently calculated values of the various  $k_{bi}$  values and of the various equilibrium constants appearing in those expressions.
71. J. Bigeleisen, M. G. Mayer, *J. Chem. Phys.* **15**, 261 (1947).
72. One effect on which we have not commented thus far is the role of collisions in stimulating vibrational energy redistribution within a molecule, a known process: In principle, some "active states" formed in the recombination, and so contributing to  $\rho_{EJ}^{\ddagger}$ , could be converted to the less active states by collision and so have their dissociative lifetime prolonged prior to the next collision. Unless the collision cross section for energy redistribution were extremely large, the calculated low-pressure results in Table 1 and Figs. 2 through 4 would be unaffected by these collisions at low pressures.
73. J. Farquhar *et al.*, *Science* **289**, 756 (2000).
74. H. Bao *et al.*, *Nature* **406**, 176 (2000).
75. M. H. Thiemens, *Science* **283**, 341 (1999).
76. ———, T. Jackson, E. C. Zipf, P. W. Erdman, C. van Egmond, *Science* **270**, 969 (1995).
77. R. Knochenmuss, *J. Phys. Chem.* **99**, 3381 (1995).
78. B. C. Hathorn, R. A. Marcus, *J. Phys. Chem. A* **105**, 5586 (2001).
79. B. Brunetti *et al.*, *J. Chem. Phys.* **74**, 6734 (1981), table I.
80. V. G. Tyuterev, S. Tashkun, P. Jensen, A. Barbe, T. Cours, *J. Mol. Spectrosc.* **198**, 57 (1999).
81. It is a pleasure to acknowledge the support of this research by the NSF and the helpful discussions with B. Hathorn in its early stages. We are very pleased to acknowledge helpful comments by K. Mauersberger, S. Anderson, M. Thiemens, R. Weston, and the reviewers.

21 December 2000; accepted 22 May 2001

Published online 31 May 2001;

10.1126/science.1058528

Include this information when citing this paper.

## Ubiquitination of a New Form of $\alpha$ -Synuclein by Parkin from Human Brain: Implications for Parkinson's Disease

Hideki Shimura,<sup>1,2\*</sup> Michael G. Schlossmacher,<sup>1,2\*†</sup>  
Nobutaka Hattori,<sup>4</sup> Matthew P. Frosch,<sup>1,2,3</sup>  
Alexander Trockenbacher,<sup>5</sup> Rainer Schneider,<sup>5</sup>  
Yoshikuni Mizuno,<sup>4</sup> Kenneth S. Kosik,<sup>1,2‡</sup> Dennis J. Selkoe<sup>1,2‡</sup>

Parkinson's disease (PD) is a common neurodegenerative disorder characterized by the progressive accumulation in selected neurons of protein inclusions containing  $\alpha$ -synuclein and ubiquitin. Rare inherited forms of PD are caused by autosomal dominant mutations in  $\alpha$ -synuclein or by autosomal recessive mutations in parkin, an E3 ubiquitin ligase. We hypothesized that these two gene products interact functionally, namely, that parkin ubiquitinates  $\alpha$ -synuclein normally and that this process is altered in autosomal recessive PD. We have now identified a protein complex in normal human brain that includes parkin as the E3 ubiquitin ligase, UbcH7 as its associated E2 ubiquitin conjugating enzyme, and a new 22-kilodalton glycosylated form of  $\alpha$ -synuclein ( $\alpha$ Sp22) as its substrate. In contrast to normal parkin, mutant parkin associated with autosomal recessive PD failed to bind  $\alpha$ Sp22. In an *in vitro* ubiquitination assay,  $\alpha$ Sp22 was modified by normal but not mutant parkin into polyubiquitinated, high molecular weight species. Accordingly,  $\alpha$ Sp22 accumulated in a non-ubiquitinated form in parkin-deficient PD brains. We conclude that  $\alpha$ Sp22 is a substrate for parkin's ubiquitin ligase activity in normal human brain and that loss of parkin function causes pathological  $\alpha$ Sp22 accumulation. These findings demonstrate a critical biochemical reaction between the two PD-linked gene products and suggest that this reaction underlies the accumulation of ubiquitinated  $\alpha$ -synuclein in conventional PD.

Parkinson's disease is a highly prevalent neurodegenerative disorder that causes progressive motor dysfunction, variable cognitive impairment, and shortened life expectancy (1). The molecular pathogenesis of PD remains unclear, but genetic factors play a role in some cases. The genes encoding parkin (2),  $\alpha$ -synuclein ( $\alpha$ S) (3, 4), and ubiquitin

carboxyl-terminal hydrolase (UCH)-L1 (5) have each been linked to familial forms of PD. Missense mutations in  $\alpha$ S or UCH-L1 cause rare, autosomal dominant forms of PD. In contrast, mutations of parkin are a relatively common cause of autosomal recessive PD (ARPD), which often has early onset (6, 7). As is the case in conventional ("idiopathic")

PD, the neuropathologic changes of parkin-linked ARPD are largely confined to the brainstem and include loss of selected neurons and local gliosis. However, the  $\alpha$ S- and ubiquitin-positive neuronal inclusions (Lewy bodies) that are a hallmark of conventional PD (8) are generally absent in parkin-linked ARPD (9-12).

Parkin consists of an NH<sub>2</sub>-terminal ubiquitin-like (Ubl) domain and a COOH-terminal RING box separated by a linker region (2, 13). The RING box encompasses three domains, termed RING1, IBR (in-between-RING), and RING2. Parkin was recently found in cell culture to act as a ubiquitin (Ub) ligase whose RING box recruits the E2 Ub conjugating enzymes, UbcH7 and UbcH8 (13-15). Ubiquitination is a vital cellular process by which a large variety of cellular proteins (targets or substrates) are conjugated with multimers of Ub, marking them for degradation by the proteasome (16). Conjugation requires a cascade of reactions that includes an E1 Ub activating enzyme, an E2 Ub conjugating enzyme, and an E3 Ub ligase. The E3 specifies both E2 recruitment and the recognition and binding of the substrate (16). As an E3 ligase, parkin conjugates Ub onto its unknown substrate(s) (designated "target X") for subsequent degradation by the proteasome (13). It has also been shown that parkin can associate with CDC-rel1 (14) and actin filaments (17) in cultured cells.

The loss of functional parkin molecules in ARPD should lead to the gradual accumulation of nonubiquitinated substrates that would otherwise be polyubiquitinated by this E3 ligase and efficiently degraded (13). In this regard, the absence of Lewy bodies in ARPD brains suggested to us that both functional parkin and its unknown target(s) may be required for the formation of Lewy bodies.

**Parkin colocalizes with  $\alpha$ -synuclein in brainstem Lewy bodies.** To test this hypothesis, we raised and purified high-affinity polyclonal antibodies to several regions of human parkin (18) and used these to probe Lewy bodies both immunohistochemically and biochemically. Staining with several antibodies to parkin (anti-parkin antibodies), e.g., HP2A [to amino acids (aa) 342-353], revealed that parkin epitopes specifically colocalized with  $\alpha$ S in subsets of classical brainstem Lewy bodies found in both PD (Fig. 1A) and the related neurodegenerative

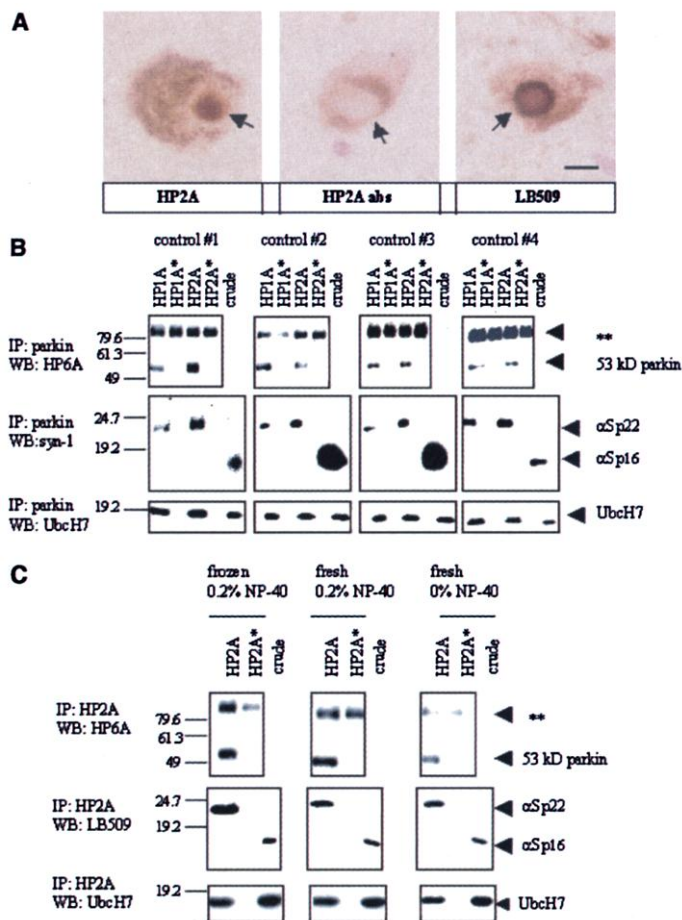
disorder, dementia with Lewy bodies (DLB) (not shown). Anti-parkin positive Lewy bodies were also detected in sections of cingulate gyrus from DLB cortex and of sympathetic gangliocytes in the peripheral autonomic nervous system from PD (18). Moreover, affinity isolated Lewy bodies were found to contain intact 53-kD neural parkin. These and related biochemical findings on the subcellular distribution of a pool of parkin,  $\alpha$ S, and UbcH7 to the same highly purified presynaptic fractions (18) led us to pursue the hypothesis that  $\alpha$ S is a key substrate for the E3 ligase activity of parkin in human brain and that disease-associated mutations in parkin prevent the ubiquitination of  $\alpha$ S.

**Wild-type parkin binds UbcH7 and a new form of  $\alpha$ -synuclein in human brain.** To determine whether parkin interacts with  $\alpha$ S in human brain, we carried out co-immunoprecipitation experiments on homogenates of frozen frontal cortex from four normal brains (19). We used parkin antibodies HP1A (to aa 84-98) and HP2A for immunoprecipitation (19), followed by immunoblotting with either parkin antibody HP6A (to aa 6-15) (18),  $\alpha$ S antibodies syn-1 and LB509, or an

antibody to UbcH7 (20). In all cases, the 53-kD parkin protein was specifically precipitated by HP1A and HP2A, whereas preabsorbed HP1A and HP2A failed to do so (Fig. 1B, top panels). The reported E2 binding partner of parkin, UbcH7 (13, 15), co-precipitated with parkin (Fig. 1B, bottom panels), as expected. HP1A and HP2A also co-precipitated a new 22-kD isoform of  $\alpha$ S (designated  $\alpha$ Sp22) but not the abundant 16-kD  $\alpha$ S monomer ( $\alpha$ Sp16), as shown by two well-characterized  $\alpha$ S antibodies, syn-1 (Fig. 1B, middle panels) and LB509 (not shown).  $\alpha$ Sp22 was never co-precipitated by preabsorbed parkin antibodies, and it was not detected when anti-parkin precipitates were blotted with syn-1 or LB509 that had been preabsorbed with recombinant human  $\alpha$ S (data not shown) (20). These immunohistochemical results were confirmed by mass spectrometry of trypsin digests of the excised  $\alpha$ Sp22 band, which yielded multiple tryptic fragments of human  $\alpha$ S (21).

To determine whether the observed association of parkin and  $\alpha$ Sp22 was influenced by freezing of the human tissue or by the use of detergents, we examined fresh human

**Fig. 1. Association of parkin and  $\alpha$ -synuclein in human brain. (A)** Immunohistochemistry on sections of PD substantia nigra. Intracellular Lewy bodies (arrows) are immunoreactive with anti-parkin (HP2A) and anti- $\alpha$ S (LB509) (18, 20). Competition with peptide antigen (HP2A absorbed) abolishes Lewy body staining but not the appearance of surrounding melanin granules. Bar, 10  $\mu$ m. **(B)** Brain homogenates of frontal cortex of four control cases were immunoprecipitated (IP) with parkin antibodies HP1A or HP2A. HP1A\* and HP2A\* signify preabsorption of each antibody with its corresponding parkin peptide. The precipitates were analyzed by Western blots (WB) with HP6A, syn-1, or anti-UbcH7, as indicated. "Crude" signifies an aliquot of the starting homogenate for each IP. Double asterisks indicate partially denatured immunoglobulin G (IgG). **(C)** Homogenates of either frozen or fresh frontal cortex of control #2 processed with or without 0.2% NP-40 were immunoprecipitated with HP2A (or parkin-preabsorbed HP2A\*), and the precipitates were blotted with HP6A, LB509, or anti-UbcH7, as indicated. Of note,  $\alpha$ Sp22 migration varies according to Tris-glycine gel conditions, ranging from 21 kD (10 to 20%) to 24 kD (4 to 20%).



<sup>1</sup>Center for Neurologic Diseases, <sup>2</sup>Department of Neurology, <sup>3</sup>Department of Pathology, Brigham and Women's Hospital, Harvard Medical School, Boston, MA, USA. <sup>4</sup>Department of Neurology, Juntendo University School of Medicine, Tokyo, Japan. <sup>5</sup>Institute of Biochemistry, University of Innsbruck, Innsbruck, Austria.

\*These authors contributed equally to this work.

†To whom correspondence should be addressed. E-mail: schloss@cnd.bwh.harvard.edu

‡These authors contributed equally to this work.

brain specimens obtained less than 18 hours after death (Fig. 1C). When these samples were processed in the presence or absence of 0.2% NP-40 and in parallel with a frozen specimen of the same brain, we observed indistinguishable co-precipitation of  $\alpha$ Sp22 and UbcH7 (Fig. 1C, middle and bottom panels) with parkin (Fig. 1C, top panels) in all three conditions. We conclude that in normal human brain, parkin, an E3 Ub ligase, is part of a stable protein complex that includes a known E2 protein, UbcH7, and a distinct  $\alpha$ S isoform,  $\alpha$ Sp22.

We next examined whether mutant parkin proteins from four parkin-linked ARPD brains can bind  $\alpha$ Sp22 and UbcH7. ARPD cases 1 and 2 each carry a homozygous deletion of exon 4, which should lead to premature termination of parkin at aa 143 (2, 22–24). ARPD cases 3 and 4 each carry a homozygous deletion of exon 3, which should cause premature termination of parkin at aa 96 (2, 23, 24). Therefore, because these truncated mutant parkin proteins lack the epitope (aa 342–353) recognized by HP2A, this antibody could neither immunoprecipitate nor blot mutant parkin from any of the four ARPD brains (Fig. 2A, top panels), as expected. However, when we probed aliquots of the starting ARPD homogenates (crude) with HP6A (to aa 6–15) or HP7A (to aa 51–62), our two most NH<sub>2</sub>-terminal parkin antibodies (18), we unexpectedly failed to detect any mutant parkin proteins (Fig. 2A, top panels; data not shown). Thus, the truncated parkin proteins may be unstable and rapidly degraded in the brains of these four ARPD patients. Consistent with the lack of detectable parkin immunoreactivity, HP2A immunoprecipitates of the ARPD homogenates did not contain  $\alpha$ Sp22 or UbcH7 (Fig. 2A, lower left panels). However, UbcH7 and the unmodified  $\alpha$ Sp16 monomer were readily

detected by immunoblotting of the crude ARPD brain homogenates (Fig. 2A, lower right panels), as expected.

Next, we examined the specificity of parkin versus another E3 Ub ligase of human brain for binding  $\alpha$ Sp22. A previously characterized antibody to E6-AP (25), an E3 Ub ligase that also recruits the E2 protein UbcH7 and is associated with Angelman syndrome (26, 27), was used in parallel immunoprecipitation experiments with HP2A, followed by blotting with antibody to  $\alpha$ S (anti- $\alpha$ S) LB509 or antibody to UbcH7 (anti-UbcH7). As expected, UbcH7 was co-precipitated from normal brain homogenates by the E6-AP antibody (Fig. 2B, bottom panel). In contrast, neither  $\alpha$ Sp22 nor the unmodified  $\alpha$ Sp16 were co-precipitated by the E6-AP antibody from brain homogenates (Fig. 2B, middle panel), demonstrating the specificity of the interaction between parkin and  $\alpha$ Sp22 in normal human brain.

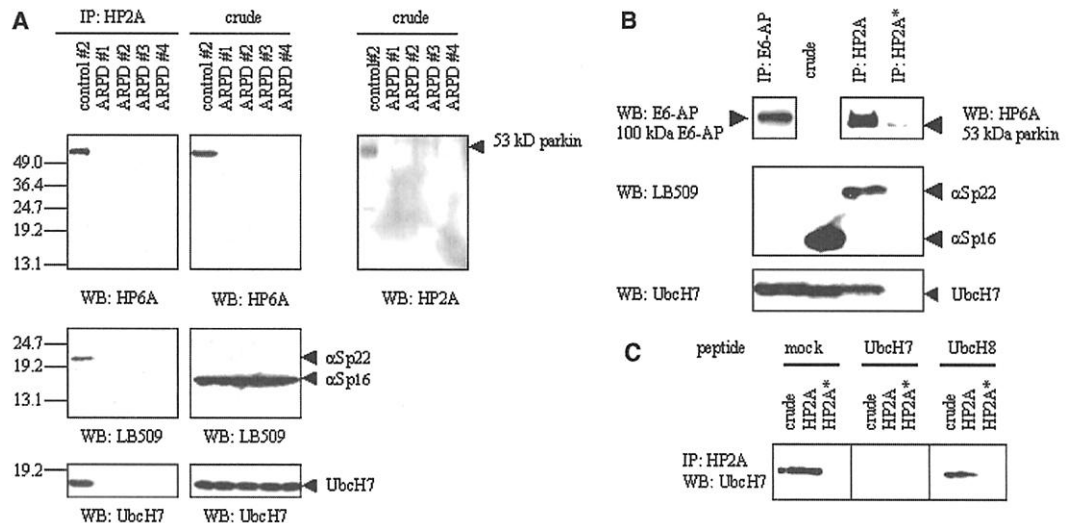
To verify the identity of the endogenous E2 protein that associates with parkin in human brain (that is, to distinguish between the highly homologous proteins UbcH7 and UbcH8), we preabsorbed aliquots of the monoclonal UbcH7 antibody with either purified, recombinant UbcH7 or UbcH8 and used them to blot HP2A immunoprecipitates (28). Only when anti-UbcH7 was preincubated with UbcH7 peptide, not with UbcH8 peptide or an irrelevant peptide, was the co-immunoprecipitated band at 17-kD abolished (Fig. 2C). These data demonstrate the specificity of anti-UbcH7 and indicate that parkin associates specifically with UbcH7 as an E2 enzyme in human brain.

**Wild-type but not mutant parkin proteins ubiquitinate  $\alpha$ Sp22.** In order to establish a functional role for parkin in human brain, we obtained immunoprecipitated (IP) parkin from frontal cortex homogenates and

tested its E3 Ub ligase activity in a previously described *in vitro* assay (Fig. 3) (13). Normal brain-derived IP parkin was incubated at 37°C for 30 min with recombinant E1, excess UbcH7 as E2, and His-tagged Ub in the presence of adenosine triphosphate (ATP) (29). The reaction products were then probed with antibody to His (anti-His) for Ub and with LB509 for  $\alpha$ S. High molecular weight (Mr) His-ubiquitinated proteins were observed in the presence of IP parkin, whereas no signal was noted in the absence of either IP parkin or E1 or UbcH7 (Fig. 3, left panels). These data confirm that endogenous parkin is an E3 Ub ligase for human brain-derived substrates, consistent with similar findings obtained in human neuroblastoma cells transfected with *myc-parkin* cDNA (13). More important,  $\alpha$ Sp22, which co-immunoprecipitated with parkin as expected, was consumed as the high Mr ubiquitinated smear appeared (detected by anti- $\alpha$ S LB509) in the presence of E1, E2, IP parkin, and ATP (Fig. 3, right panels). In contrast,  $\alpha$ Sp22 was not further modified in the absence of either E1 or UbcH7. The loss of  $\alpha$ Sp22 and simultaneous gain of the high Mr  $\alpha$ S-reactive smear of proteins during the incubation and the positive immunoreaction of the latter with both anti-His and anti- $\alpha$ S antibodies strongly suggest that these species represent, in part, polyubiquitinated forms of  $\alpha$ Sp22 [ $\alpha$ Sp22-Ub<sub>n</sub>]. Furthermore, the individual reactions shown in Fig. 3 demonstrate that brain-derived IP-parkin, in conjunction with its E2 binding partner, UbcH7, is necessary for this Ub ligase activity.

On the basis of these findings, we hypothesized that mutant parkin proteins resulting from parkin missense mutations in ARPD might fail to polyubiquitinate  $\alpha$ Sp22 for one of two reasons: (i) failure to bind  $\alpha$ Sp22 as a substrate at parkin's NH<sub>2</sub>-terminal Ubl do-

**Fig. 2.** Wild-type parkin specifically interacts with  $\alpha$ Sp22 and UbcH7 in human brain. **(A)** Lack of detection of parkin in ARPD brain. We analyzed HP2A immunoprecipitates from frontal cortex homogenates of ARPD cases #1 through 4 and control #2. The immunoprecipitates and crude extracts (starting material for the IPs) were evaluated by WB with HP2A, HP6A, LB509, or anti-UbcH7, as indicated. **(B)** Homogenates of normal human brain (control #2) were immunoprecipitated with antibodies to E6-AP or parkin (HP2A or preabsorbed HP2A\*). The precipitates were immunoblotted with anti-E6-AP, HP6A, LB509, or anti-UbcH7 as indicated. **(C)** HP2A immunoprecipitates of normal brain were analyzed by Western blot with anti-UbcH7 that was either unabsorbed (unrelated peptide), or preabsorbed with recombinant UbcH7 or UbcH8.



main or (ii) failure to recruit parkin's E2 binding partner, UbcH7, at its COOH-terminal RING box. Therefore, we generated recombinant myc-parkin Arg<sup>42</sup> → Pro<sup>42</sup> (R42P) with the Arg to Pro mutation in the Ubl domain and recombinant myc-parkin Thr<sup>240</sup> → Arg<sup>240</sup> (T240R) with the Thr to Arg mutation in the RING1 domain (30), in addition to wild-type myc-parkin (Fig. 4A). These parkin proteins were each expressed in transiently transfected HEK293 cells, immunoprecipitated with antibody to myc (Fig. 4B), and added to homogenates of frontal cortex from normal human brain. Exogenously expressed wild-type parkin was able to bind both  $\alpha$ Sp22 (Fig. 4C) and UbcH7 (Fig. 4D). In contrast, myc-parkin R42P was able to recruit UbcH7 but not  $\alpha$ Sp22, and myc-parkin T240R recruited  $\alpha$ Sp22 but not UbcH7 (Fig. 4, C and D). These findings are consistent with the reported inability of myc-parkin T240R to mediate recruitment of UbcH7 and the inability of myc-parkin R42P to interact with "target X" in cultured neuroblastoma cells (13). Furthermore, the mutant parkin proteins also failed to generate  $\alpha$ Sp22-Ub<sub>n</sub> conjugates. The IP-myc-parkin proteins were mixed with homogenates of normal frontal cortex and incubated at 37°C for 30 min with recombinant E1, UbcH7 as E2, and His-Ub in the presence of ATP (29). In this reaction, only wild-type IP-myc-parkin conferred E3 Ub ligase activity, while the mutant IP-myc-parkin fusion proteins showed no de-

tectable Ub ligase activity (Fig. 4, E and F). We conclude that exogenously generated wild-type but not ARPD-associated mutant myc-parkin, when added to human brain, can confer in vitro assembly of the myc-parkin/UbcH7/ $\alpha$ Sp22 complex as well as E3 Ub ligase activity that posttranslationally modifies  $\alpha$ Sp22.

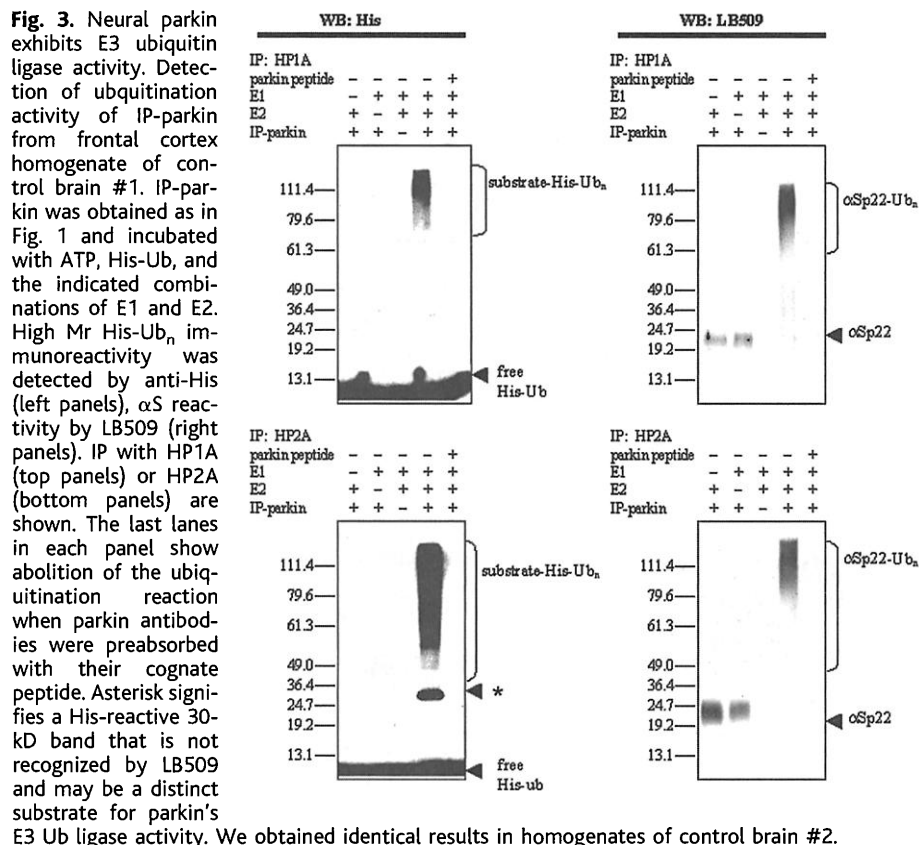
**$\alpha$ Sp22 accumulates in parkin-deficient ARPD brain.** Our findings raised the possibility of abnormal substrate ( $\alpha$ Sp22) accumulation in parkin-linked ARPD brains. To investigate this question, we first affinity-enriched for endogenous  $\alpha$ S isoforms in normal and four parkin-deficient ARPD brains (Fig. 5). Immunoprecipitates obtained with the polyclonal anti- $\alpha$ S antibody, KC7071 (20), were analyzed by blotting with anti- $\alpha$ S LB509. Under these experimental conditions, we detected  $\alpha$ Sp22 solely in ARPD brains, while the regular  $\alpha$ Sp16 monomer (KC7071's actual antigen) was seen in large and comparable amounts in both ARPD and normal tissue (Fig. 5A, upper left panel). Neither  $\alpha$ S isoform was precipitated from ARPD brain (case #2) by preimmune serum (Fig. 5A, upper right panel). These data suggested that  $\alpha$ Sp22 accumulates in ARPD brains relative to control brains, whereas the amount of unmodified  $\alpha$ Sp16 remains similar. To confirm this observation, we performed parallel pull-down assays (as described in Fig. 4C) by adding aliquots of wild-type IP myc-parkin to ARPD and con-

trol homogenates. After immunoblotting with LB509, we detected increased amounts of  $\alpha$ Sp22 in all four ARPD brains when compared with the co-migrating  $\alpha$ Sp22 species pulled down from the four control brains and the PD and DLB brains (Fig. 5A, lower panel). Therefore, the genetically and biochemically documented loss of parkin protein in our ARPD brains leads to the specific accumulation of its target substrate,  $\alpha$ Sp22. We believe that the low amounts of  $\alpha$ Sp22 in non-ARPD brains and its interaction with endogenous parkin prevented our conventional  $\alpha$ S antibody from precipitating it in sufficient amounts to be visible on Western blots.

**$\alpha$ Sp22 is an O-linked glycosylated isoform of  $\alpha$ -synuclein.** To test whether  $\alpha$ Sp22 was a mono-ubiquitinated form of  $\alpha$ S arising as a parkin-independent intermediate in polyubiquitination, we immunoblotted HP2A precipitates of normal human brain, which contained  $\alpha$ Sp22, with LB509 and anti-Ub (Fig. 5B).  $\alpha$ Sp22 was detected by LB509, as expected, but not by the Ub antibody, providing no evidence that  $\alpha$ Sp22 is mono-ubiquitinated. Treatment of the HP2A immunoprecipitates with protein phosphatase-1 did not alter the electrophoretic mobility of  $\alpha$ Sp22, and N-glycosidase treatment likewise had no effect (Fig. 5C) (31). However, co-incubation with O-glycosidase and sialidase A shifted the 22-kD species to a 16-kD position (31), where it now co-migrated with the unmodified  $\alpha$ S monomer,  $\alpha$ Sp16, from crude brain extracts (Fig. 5C). We conclude from our data obtained by mass spectrometry analysis (21) and these enzymatic digestions that  $\alpha$ Sp22 is a posttranslationally modified form of human  $\alpha$ S containing O-linked sugars.

**Discussion.** This study has uncovered a direct functional relation in human brain between the two principal gene products associated to date with inherited, monogenic forms of PD, parkin and  $\alpha$ S. The data identify a multimeric ubiquitination complex that contains a novel, O-glycosylated  $\alpha$ S isoform,  $\alpha$ Sp22, as an Ub-accepting substrate for parkin. We confirm that neural parkin is an E3 Ub ligase and show that wild-type parkin, but not mutant parkin from four previously genotyped ARPD brains, binds  $\alpha$ Sp22 and the necessary E2 protein, UbcH7, in vivo and generates high Mr species of  $\alpha$ Sp22-Ub<sub>n</sub> conjugates in vitro. Such polyubiquitination is known to serve as a universal signal for degradation by the proteasome (16) (Fig. 6).

Our findings also provide a dynamic in vitro assay for the molecular effects of naturally occurring parkin missense mutations. Exogenously expressed myc-parkin, when added to human brain homogenates in vitro, confers not only the assembly of the myc-parkin/UbcH7/ $\alpha$ Sp22 complex but also E3 Ub ligase activity. Mutant myc-parkin iso-



forms carrying ARPD missense mutations in the Ubl domain (R42P) or the RING1 domain (T240R) fail to do so, because of an inability to bind either the substrate ( $\alpha$ Sp22) or UbcH7, respectively (Figs. 4 and 6).

Such specificity of Ub ligases for their substrate(s) and E2 protein(s) is principally determined by at least two domains of the E3 protein (32). Parkin's specificity for its substrate in human brain is demonstrated by the failure of E6-AP, a non-PD related neural E3 ligase, to bind  $\alpha$ Sp22, despite the shared ability of both ligases to recruit UbcH7. Thus, the Ubl domain appears to be the principal motif that confers selectivity for parkin's target substrate(s) in vivo. Nevertheless, other motifs (for example, within the linker region) may contain alternate substrate recognition sites. It is likely that parkin has additional physiological targets in normal brain besides  $\alpha$ Sp22 (18), of which some may also contribute to the pathogenesis of PD. Of note, we did not detect co-immunoprecipitation of neural parkin and  $\beta$ -synuclein (33), a close homolog of  $\alpha$ S (not shown), or human parkin and  $\alpha$ Sp16, in our assays. Such remarkable specificity of an E3 ligase in recognizing a modified isoform (but not unmodified or homologous proteins) as substrate has been observed with other E3 ligase/substrate interactions [e.g. (34, 35)]. As concerns the RING box-mediated recruitment of parkin's E2 protein, our data identify UbcH7 as a binding partner for parkin in the  $\alpha$ Sp22-containing complex (Fig. 2). However, this finding does not preclude the possibility of parkin's interaction with other E2 proteins, an assumption that is strengthened by the localization of a sizeable pool of neural parkin in postsynaptic terminals of adult brain, where no UbcH7 (or  $\alpha$ S) can be detected (18).

The loss of normal parkin expression and thus function in ARPD leads to the accumulation of  $\alpha$ Sp22, as documented by two distinct approaches in all four of the parkin-genotyped ARPD brains analyzed by us (Fig. 5A). In the first and more direct approach, we detected  $\alpha$ Sp22 only in ARPD brains owing to the relatively low affinity of anti- $\alpha$ S KC7071 for  $\alpha$ Sp22 (but not for its cognate antigen,  $\alpha$ Sp16) under nondenaturing conditions and the overall low amount of  $\alpha$ Sp22 in normal brain (Fig. 5A, upper panels). Second, using myc-parkin proteins added to the homogenates in indirect pull-down assays, we demonstrated an increase of  $\alpha$ Sp22 in ARPD brains when compared with that pulled down from normal brains. The development of specific antibodies with high affinity for this modified *O*-glycosylated form will determine whether  $\alpha$ Sp22 also accumulates in subtle amounts in conventional PD and DLB cases (Fig. 5A, lower panel). In this regard, we have also observed a 22- to 24-kD  $\alpha$ S-immunoreactive band in extracts of affinity-isolated Lewy bodies from DLB cortex (18), rais-

ing the possibility that both  $\alpha$ Sp22 as substrate and parkin as its processing enzyme are present in ubiquitinated  $\alpha$ S inclusions (Fig. 6).

Several observations are now consistent with the conclusion that functional parkin molecules contribute to the formation of Lewy bodies in human brain: (i) the general absence of Lewy bodies in parkin-deficient ARPD brains (9-12), (ii) the presence of polyubiquitinated  $\alpha$ S in Lewy bodies (36), (iii) the presence of parkin protein in Lewy bodies (Fig. 1A) (18), and (iv) parkin's ubiquitin ligase function and the resultant generation of  $\alpha$ Sp22-Ub<sub>n</sub> conjugates (see above).

Taken together, our findings in normal and ARPD brains raise the possibility that the inherited and conventional (idiopathic) forms of PD involve etiologically distinct but biochemically related alterations of a shared metabolic pathway. In this hypothetical model, the loss of E3 ligase function (that is, parkin) in ARPD brain leads to the accumulation of nonubiquiti-

nated  $\alpha$ Sp22, accelerated neuronal loss and a generally younger age of disease onset (2, 6, 7). In contrast, in conventional Lewy body-positive PD, wild-type parkin mediates the formation of polyubiquitinated substrates, including  $\alpha$ Sp22-Ub<sub>n</sub>. Some of these  $\alpha$ Sp22-Ub<sub>n</sub>-conjugates are not efficiently processed by proteasomal degradation, perhaps due to other genetically or environmentally determined causes, and, thus, gradually accumulate (with other proteins) as inclusions in Lewy bodies (37, 38). In this regard, it is notable that the only other nuclear gene defect linked to the classical PD phenotype to date occurs in *uch-11* (5).

Such a scenario shows striking parallels to emerging information about the pathogenesis of polyglutamine expansion mutations in the spinocerebellar ataxin-1 gene, *sca-1*. Transgenic mice expressing the SCA-1[Q<sub>82</sub>] mutant develop nuclear inclusions of insoluble, polyubiquitinated SCA-1[Q<sub>82</sub>] in cerebellar Purkinje cells (39). However, the phenotype of these mice is altered when they are crossed

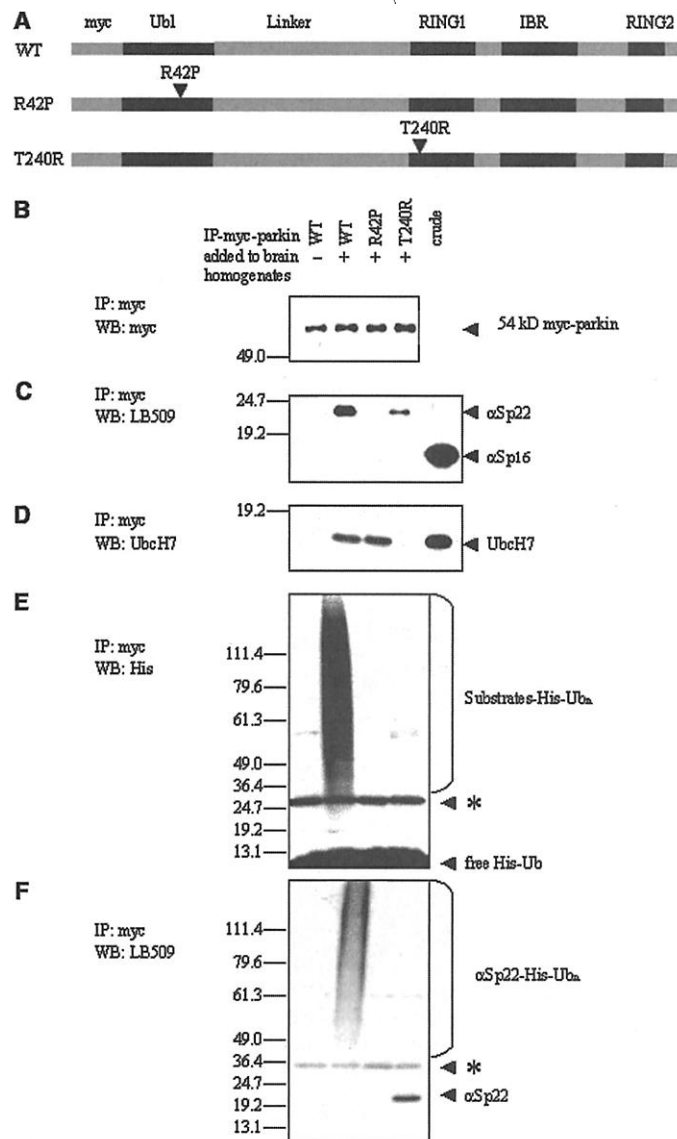


**Fig. 4.** Myc-parkin fusion proteins interact with  $\alpha$ Sp22 and UbcH7 from normal brain. **(A)** Diagrams of wild-type (WT) and R42P and T240R mutant parkin proteins. **(B, C, and D)** Myc-tagged wild-type and mutant human parkin proteins were expressed in HEK293 cells. Extracts (10 mg) were immunoprecipitated with anti-myc (13). The immunoprecipitates were incubated with (+) or without (-) frontal cortex homogenates (control case #1), washed and analyzed by WB with anti-myc (9E10) (B), anti- $\alpha$ S LB509 (C), or anti-UbcH7 (D). **(E and F)** Exogenous myc-parkin exhibits Ub ligase activity and conjugates His-Ub onto  $\alpha$ S as  $\alpha$ Sp22 is consumed (in vitro ubiquitination assay performed as in Fig. 3). Asterisk signifies non-specific bands. We obtained identical results in homogenates of control brain #2.

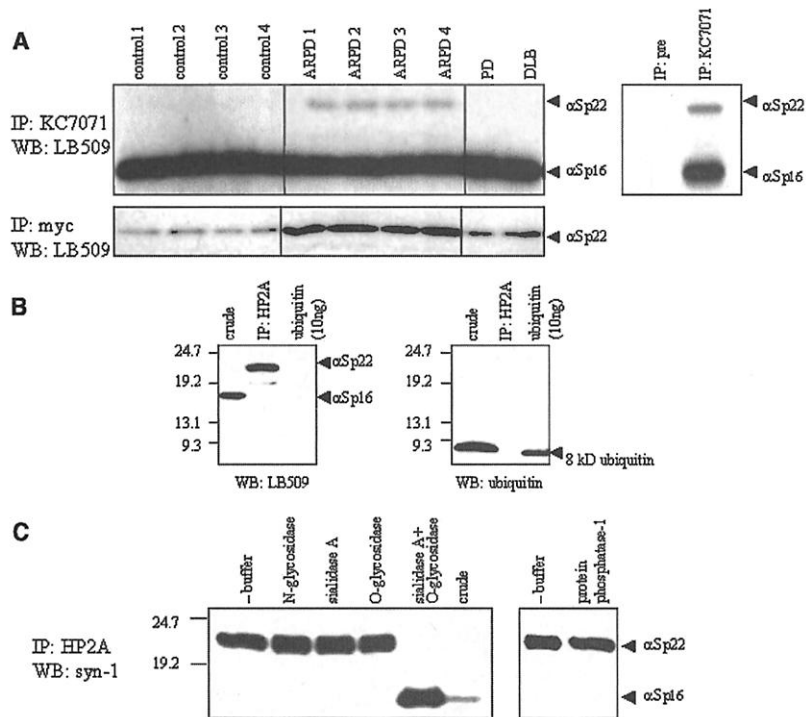


**Fig. 5.**  $\alpha$ Sp22, a glycoprotein, accumulates in ARPD brains. (A) Upper panel, anti- $\alpha$ S KC7071 immunoprecipitates obtained from 500  $\mu$ g of frontal cortex homogenates of control cases #1 through 4, ARPD brains #1 through 4, one patient with PD, and one with dementia with Lewy bodies (DLB) were blotted with anti- $\alpha$ S LB509. Right panel (ARPD case #2) shows specificity. Lower panel, anti-myc pull-down assay (performed as in Fig. 4C) of myc-parkin added to 500  $\mu$ g of brain homogenates from the same cases as in the upper panel and blotted with LB509. (B)  $\alpha$ Sp22 is not mono-ubiquitinated. Frontal cortex homogenate (crude), HP2A immunoprecipitate, and recombinant Ub were each blotted with LB509 (left panel) or anti-Ub (right panel). (C)  $\alpha$ Sp22 is O-glycosylated. HP2A immunoprecipitates (each from 2 mg normal brain homogenate) were incubated with either buffer, N-glycosidase, sialidase A, O-glycosidase, sialidase A + O-glycosidase, or protein phosphatase-1 (37), as indicated, and blotted with syn-1.

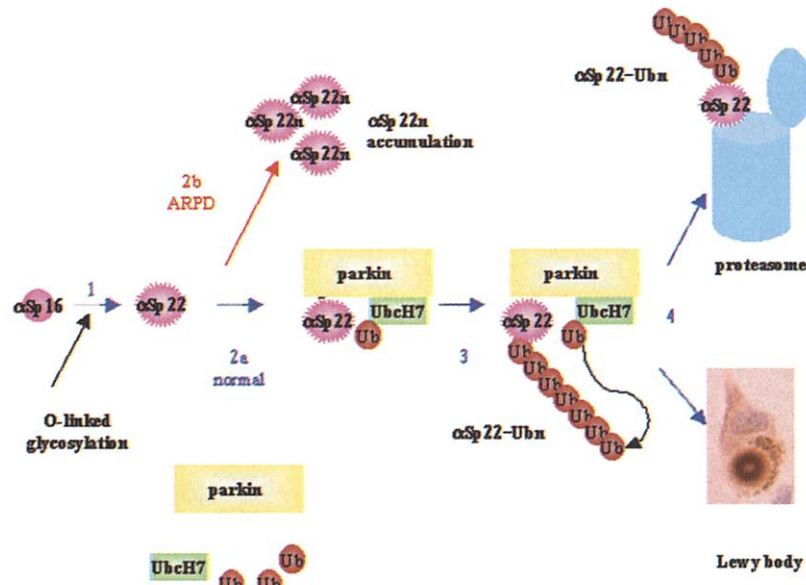


**Fig. 6.** Working model for the interaction of parkin with  $\alpha$ Sp22 in human brain. Step 1,  $\alpha$ Sp16 undergoes a posttranslational modification by the addition of O-linked sugars to generate  $\alpha$ Sp22. Step 2a, human parkin recruits UbcH7 at its RING box domain, and thus E1 protein and Ub, and binds  $\alpha$ Sp22 at its Ubl domain. Step 3, parkin conjugates Ub onto  $\alpha$ Sp22 to generate  $\alpha$ Sp22-Ub<sub>n</sub>. Step 4,  $\alpha$ Sp22-Ub<sub>n</sub> undergoes proteasomal degradation and/or sequestration in Lewy bodies (stained with anti-parkin HP2A). Interference with step 2a will lead to accumulation of  $\alpha$ Sp22<sub>n</sub> in ARPD (step 2b) and lack of  $\alpha$ Sp22-Ub<sub>n</sub> formation.

with mice lacking the gene for E6-AP Ub ligase (39). Although the degree of SCA-1[Q<sub>82</sub>]-containing nuclear inclusions is markedly decreased when the cognate E3 ligase (E6-AP) is absent, cerebellar neurons actually show augmented neuronal injury, and the mice undergo earlier neurological impairment (39). This murine model of accelerated neurodegeneration associated with defective ubiquitination and altered proteasomal degradation offers intriguing parallels to the genetic, neuropathological, and biochemical features of idiopathic and inherited PD. Future work will determine whether soluble, O-glycosylated  $\alpha$ Sp22 mediates specific physiological functions [as found for other O-glycosylated cytoplasmic proteins (40)] and/or has neurotoxic effects in PD. Of equal interest is to examine whether inherited missense mutations in  $\alpha$ S (3, 4) as well as the unknown precipitants of idiopathic PD dysregulate the metabolic pathway described here.

**References and Notes**

1. A. E. Lang, A. M. Lozano, *N. Engl. J. Med.* **339**, 1044 (1998).
2. T. Kitada *et al.*, *Nature*, **392** 605 (1998).
3. M. H. Polymeropoulos *et al.*, *Science* **276**, 2045 (1997).
4. R. Krüger *et al.*, *Nature Genet.* **18**, 106 (1998).
5. E. Leroy *et al.*, *Nature* **395**, 451 (1998).
6. C. B. Lücking *et al.*, *N. Engl. J. Med.* **342**, 1560 (2000).
7. N. Hattori *et al.*, *J. Neural Transm. Suppl.* 101 (2000).
8. M. G. Spillantini *et al.*, *Nature* **388**, 839 (1997).
9. H. Takahashi *et al.*, *Neurology* **44**, 437 (1994).
10. H. Mori *et al.*, *Neurology* **51**, 890 (1998).
11. S. Hayashi *et al.*, *Mov. Disord.* **15**, 884 (2000).
12. B. P. van de Warrenburg *et al.*, *Neurology* **56**, 555 (2001).
13. H. Shimura *et al.*, *Nature Genet.* **25**, 302 (2000).
14. Y. Zhang *et al.*, *Proc. Natl. Acad. Sci. U.S.A.* **97**, 13354 (2000).
15. Y. Imai, M. Soda, R. Takahashi, *J. Biol. Chem.* **275**, 35661 (2000).
16. K. Tanaka, T. Suzuki, T. Chiba, *Mol. Cell.* **8**, 503 (1998).
17. D. P. Huynh, D. R. Scoles, T. H. Ho, M. R. Del Bigio, S. M. Pulst, *Ann. Neurol.* **48**, 737 (2000).
18. M. G. Schlossmacher *et al.*, in preparation.
19. Frontal cortex specimens (2 g) from human brain [normal, n = 4; PD, n = 1; DLB, n = 1, collected at the Brigham and Women's Hospital brain bank (18); and ARPD, n = 4, collected at the Departments of Neurology and Pathology, Juntendo University School of Medicine] were homogenized using three volumes lysis buffer containing 0.2% NP-40 [W. Xia, *et al.*, *Proc. Natl. Acad. Sci. U.S.A.* **94**, 8203 (1997)] with EDTA-free protease inhibitors (Roche, Mannheim, Germany) and sedimented at 20,000g for 30 min at 4°C. Supernatants were incubated with antibodies ( $\pm$  peptide immunogen or control peptide) at 4°C for 1 hour. Protein A-Sepharose (20  $\mu$ l) (Sigma, St. Louis, MO) was added, followed by spinning at 2000g for 5 min, washing three times in PBS, and extraction in 4X SDS/ $\beta$ -ME sample buffer at 22°C. PAGE was performed on 4 to 20% or 10 to 20% gradient Tris glycine gels (Invitrogen, Carlsbad, CA). Proteins were transferred to PVDF membranes (Millipore, Bedford, MA) and visualized by ECL (NEN, Boston, MA).
20. Monoclonal anti- $\alpha$ S antibody LB509 was from Zymed (South San Francisco, CA); syn-1 and anti-UbcH7 from Transduction Laboratories (Lexington, KY); anti-Ub from Molecular Biological Laboratories (Nagoya, Japan); anti-His from Novagen (Madison, WI); anti-myc from Santa Cruz Biotechnology (Santa Cruz, CA). Polyclonal anti- $\alpha$ S antibody, KC7071, and its antigen, bacterially expressed and purified full-length human

- $\alpha$ S, were obtained from P. T. Lansbury [J. C. Rochet *et al.*, *Biochemistry* **39**, 10619 (2000)].
21. The silver-stained band at 22 kD in an HP2A immunoprecipitate of normal human brain and a co-migrating silver-negative slice from an adjacent lane of a parkin-preabsorbed HP2A precipitate were excised, trypsin digested and subjected to blind analysis by mass spectrometry at MDS Proteomics, Inc. (Toronto, ON) [A. Shevchenko *et al.*, *Anal. Chem.* **68**, 850 (1996)]. The HP2A-specific 22-kD protein yielded tryptic peptides corresponding to aa 13–21, 44–58, 46–58, 59–80, 61–80, 81–96, and 81–97 of human  $\alpha$ S (GenBank accession # L08850), each ending with a lysine, as expected. No  $\alpha$ S sequence was detected in the co-migrating slice from the preabsorbed lane.
  22. Y. Mizuno, N. Hattori, H. Mori, *Biomed. Pharmacother.* **53**, 109 (1999).
  23. H. Shimura *et al.*, *Ann. Neurol.* **45**, 668 (1999).
  24. N. Hattori *et al.*, *Ann. Neurol.* **44**, 935 (1998).
  25. A. L. Talis, J. M. Huijbregtse, P. M. Howley, *J. Biol. Chem.* **273**, 6439 (1998).
  26. M. Scheffner, J. M. Huijbregtse, R. D. Vierstra, P. M. Howley, *Cell* **75**, 495 (1993).
  27. Y. Jiang, E. Lev-Lehman, J. Bressler, T. F. Tsai, A. L. Beaudet, *Am. J. Hum. Genet.* **65**, 1 (1999).
  28. Human UbcH7 and UbcH8 were expressed in M15 *E. coli* harboring the *Lac*-repressor expressing plasmid pREP4, using the QIA express system (QIAGEN, Valencia, CA) with an NH<sub>2</sub>-terminal 6xHis tag. Proteins were purified on nickel NTA-agarose (QIAGEN). Enzymatic activity was tested in Ub shift assays.
  29. Parkin was immunoprecipitated (yielding IP-parkin) from frontal cortex homogenates or HEK293 cells transiently transfected with myc-parkin cDNA (10  $\mu$ g) (73). IP parkin was incubated at 37 °C in 50  $\mu$ l of reaction buffer containing ATP (4 mM ATP in 50 mM Tris-HCl, pH 7.5, 2 mM MgCl<sub>2</sub>), 100 ng of recombinant human E1, 2  $\mu$ g of UbcH7 (E2), and 2  $\mu$ g His-Ub (all from Affinity Research Products, Exeter, UK). The reaction was terminated by adding 20  $\mu$ l of 4X sample buffer, and 25  $\mu$ l aliquots of the reaction mixtures were electrophoresed and immunoblotted.
  30. We prepared WT and ARPD-mutant parkin cDNAs [N. Hattori *et al.*, *Biochem. Biophys. Res. Commun.* **249**, 754 (1998); L. Terreni *et al.*, *Neurology* **56**, 463 (2001)] in a pcDNA3.1(+) vector using the QuikChange site-directed mutagenesis kit (Stratagene, La Jolla, CA) and transiently transfected them into HEK293 cells using Lipofectamine 2000 (Gibco, Rockville, MD), as per manufacturers' instructions.
  31. For enzymatic digestion of HP2A precipitates, *N*-glycosidase, sialidase A, endo-O-glycosidase [with bovine fetuin as a control protein (ProZyme, San Leandro, CA)], and protein phosphatase-1 (Sigma) were used as per manufacturers' instructions.
  32. C. A. Joazeiro, A. M. Weissman, *Cell* **102**, 549 (2000).
  33. P. J. Kahle *et al.*, *J. Neurosci.* **20**, 6365 (2000).
  34. M. Ivan *et al.*, *Science* **292**, 464 (2001).
  35. P. Jaakkola *et al.*, *Science* **292**, 468 (2001).
  36. J. Q. Trojanowski, M. Goedert, T. Iwatsubo, V. M. Lee, *Cell Death Differ.* **5**, 823 (1999).
  37. M. S. Goldberg, P. T. Lansbury, *Nature Cell Biol.* **2**, E115 (2000).
  38. N. F. Bence, R. M. Sampat, R. R. Kopito, *Science* **292**, 1552 (2001).
  39. C. J. Cummings *et al.*, *Neuron* **24**, 879 (1999).
  40. L. Wells, K. Vosseller, G. W. Hart, *Science* **291**, 2376 (2001).
  41. We thank H. Mori, Y. Mizutani, and K. Yamane for ARPD brain specimens; J. Chan for providing normal human brain; and the patients' families for the donation of tissue. We also thank K. Wynn and P. Howley for anti-E6-AP (JH-16), T. Suzuki and K. Tanaka for a parkin cDNA-containing vector, P. Lansbury for reagents and critical review of our manuscript, and M. Medina for experimental advice. H.S. is supported by a Pergolide Fellowship (Eli Lilly, Japan K.K.). M.G.S. is supported by the Grass Foundation (Robert S. Morison Fellowship), the Lefler Foundation, and the NIH (NS 02127). M.P.F. is supported by a Beeson Scholar Award. R.S. received grants from the National Bank of Austria. Supported by the Morris R. Udall Center of Excellence in PD (NS 38375) at Brigham and Women's Hospital (M.P.F., K.S.K., and D.J.S.).

12 March 2001; accepted 6 June 2001

Published online 28 June 2001;

10.1126/science.1060627

Include this information when citing this paper.

## REPORTS

## Visible-Light Photocatalysis in Nitrogen-Doped Titanium Oxides

R. Asahi,\* T. Morikawa, T. Ohwaki, K. Aoki, Y. Taga

To use solar irradiation or interior lighting efficiently, we sought a photocatalyst with high reactivity under visible light. Films and powders of TiO<sub>2-x</sub>N<sub>x</sub> have revealed an improvement over titanium dioxide (TiO<sub>2</sub>) under visible light (wavelength < 500 nanometers) in optical absorption and photocatalytic activity such as photodegradations of methylene blue and gaseous acetaldehyde and hydrophilicity of the film surface. Nitrogen doped into substitutional sites of TiO<sub>2</sub> has proven to be indispensable for band-gap narrowing and photocatalytic activity, as assessed by first-principles calculations and x-ray photoemission spectroscopy.

Since photoinduced decomposition of water on TiO<sub>2</sub> electrodes was discovered (1), semiconductor-based photocatalysis has attracted extensive interest. One particular focus has been on applications in which organic molecules are photodegraded, such as water and air purifications (2–4). Most of the investigations have focused on TiO<sub>2</sub> (5–7), which shows relatively high reactivity and chemical stability under ultraviolet (UV) light [wavelength ( $\lambda$ ) < 387 nm], whose energy exceeds the band gap of 3.2 eV in the anatase crystalline phase.

The development of photocatalysts that can yield high reactivity under visible light ( $\lambda$  >

380 nm) should allow the main part of the solar spectrum, and even poor illumination of interior lighting, to be used. One approach has been to dope transition metals into TiO<sub>2</sub> (8–10), and another has been to form reduced TiO<sub>x</sub> photocatalysts (11, 12). However, doped materials suffer from a thermal instability (9), an increase of carrier-recombination centers, or the requirement of an expensive ion-implantation facility (10). Reducing TiO<sub>2</sub> introduces localized oxygen vacancy states located at 0.75 to 1.18 eV below the conduction band minimum (CBM) of TiO<sub>2</sub> (12), so that the energy levels of the optically excited electrons will be lower than the redox potential of the hydrogen evolution (H<sub>2</sub>/H<sub>2</sub>O) located just below the CBM of TiO<sub>2</sub> (13) and that the electron mobility in the bulk region will be small because of the localization.

We have considered whether visible-light

activity could be introduced in TiO<sub>2</sub> by doping, and we set the following requirements: (i) doping should produce states in the band gap of TiO<sub>2</sub> that absorb visible light; (ii) the CBM, including subsequent impurity states, should be as high as that of TiO<sub>2</sub> or higher than the H<sub>2</sub>/H<sub>2</sub>O level to ensure its photoreduction activity; and (iii) the states in the gap should overlap sufficiently with the band states of TiO<sub>2</sub> to transfer photoexcited carriers to reactive sites at the catalyst surface within their lifetime. Conditions ii and iii require that we use anionic species for the doping rather than cationic metals, which often give quite localized *d* states deep in the band gap of TiO<sub>2</sub> and result in recombination centers of carriers. We have calculated densities of states (DOSs) of the substitutional doping of C, N, F, P, or S for O in the anatase TiO<sub>2</sub> crystal, by the full-potential linearized augmented plane wave (FLAPW) formalism (14, 15) in the framework of the local density approximation (LDA) (16) (Fig. 1). The substitutional doping of N was the most effective because its *p* states contribute to the band-gap narrowing by mixing with O *2p* states. Although doping with S shows a similar band-gap narrowing, it would be difficult to incorporate it into the TiO<sub>2</sub> crystal because of its large ionic radius, as evidenced by a much larger formation energy required for the substitution of S than that required for the substitution of N (17). The states introduced by C and P are too deep in the gap to satisfy condition iii. The calculated imaginary parts of the dielectric functions of TiO<sub>2-x</sub>N<sub>x</sub> indeed show a shift of the absorption edge to a lower energy by the N doping (Fig. 2A) (18). Dominant transitions at the absorption edge have been identified with

Toyota Central R&D Laboratories, Nagakute, Aichi 480-1192, Japan.

\*To whom correspondence should be addressed. E-mail: rasahi@mosk.tytlabs.co.jp